CONSTRAINTS ON MARTIAN AEROSOLS FROM TES IR OBSERVATIONS: SIZES AND SHAPES.

M. J. Wolff, R. T. Clancy, *Space Science Institute, Boulder, CO, USA (wolff@colorado.edu).*

Introduction

The roles of aerosols in the Mars atmosphere and climate are fundamental on several levels. Even prior to the seminal Mariner 9 mission, radiative forcing from atmospheric dust solar absorption and thermal emission was recognized as a primary factor in the thermal structure of the global Mars atmosphere [7]. Mariner 9 and Viking observations during the intense global dust storm seasons of 1971 and 1977 identified the strong, vertically deep, and very abrupt forcing on global circulation associated with perihelion dust storm activity [16, 9]. It has also been proposed that the non-linear microphysics of dust-ice aerosol interactions plays an active role in the latitudinal and annual variations of aerosol and water vapor distributions and their cross-hemispheric transport [5]. Of key importance in addressing such issues is the seasonally/spatially variable aerosol composition (ice and dust components), particle sizes and shapes. A combination of recent improvements in numerical methods and hardware performance with the dataset returned by the Mars Global Surveyor Thermal Emission Spectrometer (TES) have finally made the investigation of these parameters reasonably tractable. This presentation focusses on the specific aspect of particle size and shape, although only details of the former are presented in this abstract.

Data

The TES IR spectral data analyzed here are taken from the so-called "emission phase function" (EPF) sequences. Details of this type of observation are given in ([6] and references within. In essence, a specific location on the surface is observed at various emission angles as the spacecraft passes over it. The sampling scheme of these data is such that one can, in principle, obtain additional leverage on both surface and atmospheric properties relative to that from nadir data. However, the combination of pointing drift (e.g., [2]) and non-uniform surface emissivity (i.e., emission phase function is not Lambertian) provide sufficient motivation to confine our analyses to the nadir observations.

A description of the TES instrument and its calibration characteristics may be found in numerous recent publications. The interested reader is referred to recent report of [3], where a very complete description of TES and its data products is given. For our purposes, it is sufficient to indicate that our spectra are a coaddition of all six detectors for each integration (i.e., ICK). Error propagation includes the 1-σ Noise Equivalent Radiance values for a single detector (2.5×10^{-8} W cm^{-2} sr^{-1} cm^{-1}from 300 cm^{-1} to 1400 cm^{-1}; 6×10^{-8} W cm^{-2} sr^{-1} cm^{-1}at 250 cm^{-1}; 4×10^{-8} W cm^{-2} sr^{-1} cm^{-1}at 1450 cm^{-1}; linear interpolation used for 250-300 cm^{-1} and 1450-1600 cm^{-1} ranges) added in quadrature with a background radiance uncertainty (1×10^{-8} W cm^{-2} sr^{-1} cm^{-1}).

Some Numerical Details

IR Radiative Transfer

Our model-data comparisons employ a modified version of doubling-adding radiative transfer code described by [4], which itself was adapted by *Clancy et al.* from the terrestial atmospheric modeling code of [8]. Our primary modifications include the option to include molecular opacity via a correlated-k algorithm (e.g., [10]), as well as the ability to easily use arbitrary surface emissivity spectra and aerosol dielectric functions. The atmospheric vertical structure is specified with a resolution of 2 km for altitudes of 0-20 km, and of 5 km for 20-60 km.

Dielectric Function

We consider only two basic aerosol materials: water ice and "dust." The dielectric function for the former is taken directly from the work of Warren and collaborators ([15]; see also ftp://climate.gsfc.nasa.gov/pub/-wiscombe/Refrac_Index/ICE/). For dust, we adopted a dielectric function that is a synthesis of recent work in the optical and thermal IR ([4] and references within; [12, 14, 13]; G. Hansen, personal communication, 2001) with modifications made during the course of our investigation. See Figure 1.

Nadir Surface Emissivity

The surface of Mars has a distinctly non-unit surface emissivity over the TES spectral region (e.g., [1]). Consequently, efforts to retrieve atmospheric particle properties may be significantly biased without an accurate representation of this important surface property. We use a nadir surface emissivity map kindly constructed for us by J. Bandfield, based upon his work cited above. The data set used in the map product was taken in 10 cm^{-1} sampling mode avoided the use of any observations containing detectable amounts of water ice. The data were corrected for dust aerosol and coadded spatially into 1°x1° bins. The spectra are clipped spectrally below 250

cm^{-1} (poor signal-to-noise), above 1300 cm^{-1} (problems with atmospheric correction, and to a lesser extent, poor signal-to-noise), and 510-820cm^{-1} (main CO_2 feature). H_2O vapor and minor/isotopic CO_2 bands remain in the maps, though the former contribution is minimized due to the temporal and spatial variability of H_2O vapor abundances (e.g., [11]).

Results

The results of our retrievals are presented in Tables 1-3. The assignment of observations to a particular type (e.g., dust, Type 1 ice, Type 2 ice) is based upon a classification using the TES solar band EPF data [6]. The uncertainties in retrieved optical depths (at the reference wavenumbers of 1075 cm^{-1} and 825 cm^{-1} for dust and ice, respectively) are generally 0.02-0.03. The uncertainties for the particle sizes are dependent upon the total column of the relevant aerosol component as well as the size itself. The TES data are most sensitive to changes in the dust sizes, where one finds r_{eff} with $\pm 0.3 - 0.4$ (for $\tau_{dust,1075} \geq 0.2$). The situation for ice is less favorable, though one is able to delineate between the two types of ice particles found from analysis of the TES solar band data [6]. For $\tau_{ice,825} \geq 0.4$, one finds r_{eff} with $(\pm 0.6 - 0.7)$; for $\tau_{ice,825}$ below this level, it is much more dependent upon the retrieved size, with the Type 1 ice being typically constrained to 1.0-2.3 μm and Type 2 to 2.5-4.0 μm.

Acknowledgements: We gratefully acknowledge the generous contributions of Josh Bandfield, Kelly Bender, Michael Mishchenko, Kim Murray, Kelly Snook, Warren Wiscombe, and the TES team at Arizona State University.

References

[1] Bandfied, J. L., Global mineral distribution on Mars, JGR, *107*, 10.1029/2001JE001510, in press, 2002.

[2] Bandfied, J. L., and M. D. Smith, Multiple emission angle surface-atmosphere separations of Thermal Emission Spectrometer, JGR, in press, 2002.

[3] Christensen, P. R. *et al.*, Mars Global Surveyor Thermal Emission Spectrometer experiment: Investigation description and surface science results, JGR, *106*, 23,823–23,871, 2001.

[4] Clancy, R. T., S. W. Lee, G. R. Gladstone, W. W. McMillan, and T. Rousch, A new model for Mars atmospheric dust based upon analysis of ultraviolet through infrared observations from Mariner 9, Viking, and Phobos, JGR *100*, 5251–5264, 1995.

[5] Clancy, R. T. et al. Water vapor saturation at low altitudes around Mars aphelion: A key to Mars climate?, Icarus *122*, 36–62, 1996.

[6] Clancy, R. T., M. J. Wolff, and P. R. Christensen,Mars aerosol atudies with the MGS TES emission phase function observations: Optical depths, particle sizes, and ice cloud types versus latitude and solar longitude, JGR, submitted, 2002.

[7] Gierasch, P.J., and R. Goody, A study of the thermal and dynamical structure of the Martian lower atmosphere, Planet. Space Sci. *16*, 615–646, 1968.

[8] Gladstone, G. R., J. W. Kaminski, R. Link, and J. C. McConnell, Cloud radiance modeling: Phase II, contract KM147-4-1041, Can. Dept. of the Environ., Ottawa, Ontario, 1984.

[9] Kahn, R., T. Z. Martin, R. W. Zurek, and S. W. Lee, The Martian Dust Cycle, in *Mars*, eds. Kieffer et al., 1017–1053 (U. Arizona Press, Tucson), 1992.

[10] Lacis, A. A.,and V. Oinas, A description of the correlated k distribution methof for modeling nongray gaseous absorption, thermal emission, and multiple scattering in vertically inhomogeneous atmosphere, JGR, *96*, 9027–9063, 1991.

[11] Smith, M. D., Annual cycle of water vapor on Mars as observed by the Thermal Emission Spectrometer, JGR, *107*, 10.1029/2001JE001522, in press, 2002.

[12] Snook, K. J., Optical properties and radiative heating effects of dust suspended in the Mars atmosphere, Ph.D Thesis, Stanford University, Stanford, California, 1999.

[13] Snook, K. J., J. L. Bandfield, F. Forget, and C. P. McKay, Derivation of infrared optical Properties of dust suspended in the martian atmosphere from MGS-TES data, BAAS, *32*, 51.08, 2000.

[14] Tomasko, M. G., L. R. Doose, M. Lemmon, E. Wegryn, and P. H. Smith, Properties of dust in the Martian atmosphere from the imager on Mars Pathfinder, JGR, *104*, 8987–9008, 1999.

[15] Warren, S., Optical constants of ice from the ultraviolet to the Microwave, Appl. Opt.,*23*, 1206–1225, 1984.

[16] Zurek, R. W., Comparative aspects of the climate of Mars: An introduction to the current atmosphere, in *Mars*, eds. Kieffer et al., 799–817 (U. Arizonal Press, Tucson), 1992.

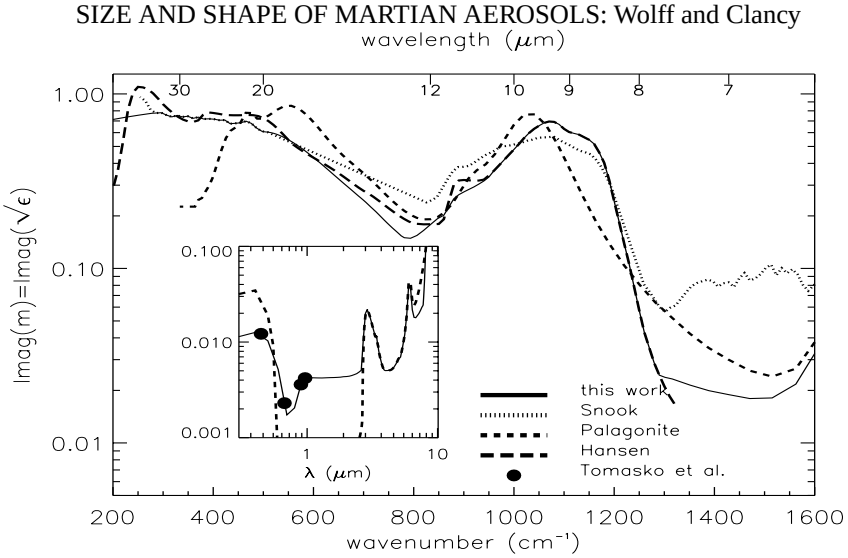

Figure 1. Comparison of the imaginary part (k) of the adopted complex indices of refraction ($m = n + ik = \sqrt{\epsilon}$) to those of the components used as initial values. The "palagonite" material is that published by [4].

Table 1. Modeled TES Data - "Dust"

						TES Team				This Work					
ock	ick	L_S (°)	emis (°)	long (°)	lat (°)	τ_d	τ_i	T_{surf} (K)	P_{surf} (mb)	τ_d	τ_i	T_{surf} (K)	$r_{eff,d}$ (μm)	$r_{eff,i}$ (μm)	Comments
3631	1803	188.2	0.6	173.4	5.9	0.16	0.04	280	6.9	0.21	0.04	220	1.8	1.6	
4242	1630	218.1	4.5	21.7	-11.8	0.25	-0.01	294	6.8	0.39	0.00	296	1.6	···	
4279	1779	219.9	0.6	2.7	3.4	0.21	0.01	284	6.6	0.32	0.02	285	1.6	1.6	
4353	2079	223.7	0.6	325.3	34.0	0.19	0.08	237	6.4	0.25	0.04	239	1.5	1.6	
4457	2774	229.0	0.6	53.6	-30.1	0.46	-0.02	290	5.4	0.68	0.00	292	1.9	···	
4545	1240	233.5	4.0	49.0	-51.6	0.49	0.00	273	7.8	0.72	0.00	275	1.6	···	
4712	3029	242.2	0.6	159.6	18.7	0.51	0.01	256	8.8	0.71	0.02	258	1.5	1.6	
5404	1306	277.9	0.6	159.4	-44.9	0.12	0.01	300	4.8	0.16	0.02	300	1.5	1.6	
5451	1161	280.2	0.6	61.4	-59.7	0.11	0.01	292	5.7	0.13	0.00	293	1.5	···	
6188	1893	316.3	0.6	288.2	9.4	0.09	0.02	295	4.9	0.13	0.00	295	1.5	···	
6392	1893	325.7	0.6	8.1	15.0	0.23	0.02	272	6.8	0.34	0.02	273	1.6	···	
7847	2340	25.9	0.6	264.8	60.1	0.15	0.04	239	8.5	0.19	0.05	240	1.5	1.6	
8241	2079	40.5	0.6	18.7	33.6	0.20	0.04	270	8.7	0.25	0.04	272	1.5	1.6	
8381	1452	45.7	0.6	58.1	-29.9	0.07	0.04	244	5.1	0.11	0.03	244	1.5	1.6	
11841	2041	179.1	0.6	171.4	29.9	0.09	0.02	274	7.2	0.17	0.02	275	1.6	1.6	
11931	2041	183.2	0.6	230.4	29.9	0.14	0.01	272	7.6	0.23	0.01	273	1.7	1.6	
12021	2031	187.5	0.6	289.5	30.1	0.75	-0.01	245	5.1	0.94	0.04	247	1.4	1.6	1
12039	1374	188.3	0.6	75.8	-38.1	0.14	0.00	274	3.6	0.26	0.00	275	2.1	···	
12051	1452	188.9	0.6	60.9	-30.1	0.24	0.00	276	4.2	0.35	0.00	277	1.9	···	
12059	1520	189.2	0.6	291.1	-22.8	1.22	0.12	244	5.7	1.59	0.04	246	2.4	1.6	
12062	1814	189.4	0.6	21.1	6.8	0.47	-0.01	273	6.6	0.66	0.00	274	1.8	···	
12148	1599	193.5	0.6	322.5	-14.8	1.23	0.01	266	4.0	1.68	0.00	269	2.0	···	
12157	2041	193.9	0.6	226.5	29.9	0.59	-0.02	252	7.7	0.81	0.00	253	1.4	···	
12322	2041	201.9	0.6	274.5	30.2	1.12	0.11	231	7.4	1.46	0.07	232	1.7	1.6	2
12397	2041	205.6	0.6	263.6	30.2	1.00	-0.03	231	8.1	1.79	0.00	234	1.6	···	
12412	2031	206.3	0.6	333.3	29.9	1.00	-0.07	230	6.3	1.61	0.05	232	1.3	1.6	2,3
12463	1599	208.9	0.6	348.5	-14.9	2.01	-0.07	253	5.1	2.49	0.00	257	1.7	···	2
12700	1452	220.7	0.6	297.3	-28.2	2.09	-0.03	250	7.3	2.45	0.03	253	1.7	1.6	2

Comments: 1 - v_{eff}=0.2; 2 - TES optical depths flagged as "questionable"; 3 - v_{eff}=0.1.

Table 2. Modeled TES Data - "Ice Type 1"

						TES Team				This Work					
ock	ick	L_S (°)	emis (°)	long (°)	lat (°)	τ_d	τ_i	T_{surf} (K)	P_{surf} (mb)	τ_d	τ_i	T_{surf} (K)	$r_{eff,d}$ (μm)	$r_{eff,i}$ (μm)	Comments
1813	1831	112.1	0.6	327.6	-2.3	0.07	0.06	266	4.3	0.08	0.08	266	1.5	1.5	
2070	1597	121.9	0.6	123.9	-15.2	0.04	0.09	249	2.4	0.04	0.12	248	1.5	1.5	
2407	1683	135.1	0.6	53.5	-6.8	0.11	0.17	265	3.9	0.06	0.25	267	1.5	2.0	
2469	1977	137.6	0.6	32.6	23.5	0.07	0.04	282	6.9	0.12	0.04	283	1.5	1.5	
2515	1683	139.4	0.6	265.7	-6.3	0.09	0.12	271	4.2	0.05	0.11	271	1.5	1.5	
2610	1595	143.3	0.6	104.4	-15.1	0.02	0.05	257	2.5	0.05	0.09	258	1.5	1.6	
4353	2081	223.7	0.6	325.3	34.0	0.19	0.08	237	6.4	0.21	0.05	238	1.5	1.7	
7337	1452	6.0	0.6	51.7	-29.8	0.14	0.04	267	5.1	0.15	0.04	267	1.5	1.6	
7805	1452	24.3	0.6	128.4	-29.9	0.02	0.03	249	4.4	0.05	0.06	250	1.5	1.8	
8549	1520	51.7	0.6	188.9	-23.1	0.04	0.04	243	5.1	0.06	0.05	244	1.5	1.5	
8598	1599	53.5	0.6	152.9	-14.6	0.05	0.08	253	5.3	0.08	0.11	255	1.5	1.5	
8876	1929	63.5	0.6	196.7	18.6	0.07	0.07	265	7.1	0.04	0.10	266	1.5	2.0	
9162	1599	73.7	0.6	101.3	-14.8	0.03	0.08	242	2.8	0.02	0.10	242	1.5	1.5	
9437	1479	83.5	0.6	54.0	-27.4	0.02	0.04	237	5.1	0.05	0.06	237	1.5	1.5	
9818	1746	97.3	0.6	168.4	0.0	0.11	0.13	260	7.1	0.08	0.15	260	1.5	1.9	
9929	1599	101.3	0.6	105.2	-15.3	0.07	0.11	241	2.8	0.08	0.15	242	1.5	1.5	

Table 3. Modeled TES Data - "Ice Type 2"

						TES Team				This Work					
ock	ick	L_S (°)	emis (°)	long (°)	lat (°)	τ_d	τ_i	T_{surf} (K)	P_{surf} (mb)	τ_d	τ_i	T_{surf} (K)	$r_{eff,d}$ (μm)	$r_{eff,i}$ (μm)	Comments
1886	1831	114.9	0.6	259.9	14.6	0.11	0.14	265	6.7	0.09	0.23	268	1.5	3.2	
2038	1831	120.7	0.6	291.2	10.8	0.09	0.17	282	4.0	0.03	0.28	285	1.5	3.3	
2056	1831	121.4	0.6	86.1	6.9	0.15	0.27	263	4.4	0.06	0.39	265	1.5	3.0	
2345	1831	132.6	0.6	81.0	12.6	0.08	0.18	271	4.9	0.05	0.25	273	1.5	3.0	
2420	1830	135.6	0.6	37.2	0.6	0.15	0.32	268	4.6	0.03	0.52	272	1.5	3.2	1
2434	2125	136.2	0.6	112.9	38.7	0.13	0.40	267	2.6	0.03	0.54	270	1.5	1.8	1
2516	1830	139.5	0.6	296.3	8.7	0.08	0.12	285	3.9	0.06	0.18	287	1.5	3.2	
8155	1780	37.4	4.5	72.6	3.5	0.10	0.16	272	4.8	0.04	0.21	274	1.5	1.8	
8180	1893	38.3	0.6	69.8	15.1	0.13	0.11	274	5.7	0.11	0.19	276	1.5	3.0	
8900	1929	64.3	0.6	163.9	18.5	0.12	0.11	266	8.2	0.07	0.15	272	1.5	2.5	
8959	1814	66.4	0.6	51.7	7.0	0.09	0.15	259	5.9	0.06	0.23	262	1.5	3.0	
8960	1962	66.5	0.6	82.3	22.0	0.09	0.12	270	5.7	0.06	0.20	273	1.5	3.0	
8986	2190	67.4	0.6	110.4	45.1	0.12	0.25	262	3.6	0.03	0.34	264	1.5	2.5	1
9391	1746	81.9	0.6	180.5	0.0	0.09	0.12	260	7.0	0.10	0.21	263	1.5	3.1	
9699	1893	92.9	0.7	2.4	14.8	0.09	0.12	268	6.3	0.08	0.21	270	1.5	3.4	
10560	1746	125.1	0.6	181.3	0.1	0.10	0.12	267	6.2	0.10	0.17	268	1.5	3.0	
10649	1962	128.5	0.6	214.0	21.9	0.18	0.38	270	4.1	0.06	0.51	273	1.5	3.3	
10740	1746	132.1	0.6	298.4	0.3	0.09	0.16	276	3.8	0.05	0.26	278	1.5	3.4	

Comments: 1 - TES optical depths flagged as "questionable".